Environ. Eng. Res. 2020; 25(5): 714-721
https://doi.org/10.4491/eer.2019.297

pISSN 1226-1025
eISSN 2005-968X

Effect of ion exchange dialysis process variables on aluminium permeation using response surface methodology

Dennis Asante-Sackey[1], Sudesh Rathilal[1], V.L Pillay[2], Emmanuel Kweinor Tetteh[1†]

[1]*Faculty of Engineering and the Built Environment, Department of Chemical Engineering, Durban University of Technology, Steve Biko Campus, Block S4 Level 1, Box 1334, Durban 4000, South Africa.*
[2]*Faculty of Engineering, Department of Process Engineering, Stellenbosch University, Matieland 7602, South Africa*

ABSTRACT

This study investigated aluminum permeation using a counter flow ion exchange dialysis (IED) system. The optimum conditions for permeation were investigated using response surface methodology (RSM). Effect of four factors- feed concentration (100-2,000 ppm, A), feed flow rate (25-85%, B), sweep concentration (0.25-1 N HCl, C) and sweep flow rate (25-85%, D) were studied using face centered central composite (FC-CCD) statistical experimental design. A RSM model was developed based on the experimental permeation data and the response plot was developed. The FC-CCD model predicted permeation correlated with the experimental data. The regression coefficient (R^2) was found to be 0.9568. The experiment showed the ascending order of the effect of the variables is D < B < C < A. In a counter flow IED for Al permeation, the sweep flow rate is insignificant ($p > 0.05$). Experimental validation demonstrated for target permeation of 70% was 68.8% ± 2.22%. This suggested that the RSM was a suitable tool in optimizing Al-permeation.

Keywords: Alum, Coagulation, Ion exchange dialysis (IED), Response surface methodology (RSM)

1. Introduction

Aluminium is the third most abundant element but the most abundant metal in the earth's crust-8.1wt % [1, 2]. Variety of Al applications are in the electrical and electronics, construction, transportation and chemical industries. In the water and wastewater treatment industry, Hydrolytic Al salt is used as a coagulant or flocculating agent in the purification of water. Notable amongst them are aluminum sulphate [$Al_2(SO_4)_3.xH_2O$], poly aluminium chloride [$Al_x(OH)_y Cl_z$], poly aluminium silicate sulphate [$Al_w(OH)_x(SO4)_y(SiO2)_z$] and sodium aluminate [$NaAlO_2$] [3-5]. The aluminium sulfate, commercially known as alum is the most widely used coagulant. These are often available in solid (block, kibbled or ground) and liquid form. The water of crystallization coefficient (x) in the solid alum ranges from 14-21 containing 14-18% w/w Al_2O_3 or 7.5-9% Al, while the liquid form contains 8% w/w Al_2O_3 or 4.2% Al [6].

Alum has a good adsorption affinity for metal ions and anions such as phosphate, fluoride and perchlorates [7]. Due to the natural alkalinity of water which is usually bicarbonate of calcium, the dosage of the acidic alum results in the formation of aluminium hydroxide (Eq. (1)). This is then precipitated out with particulate matter as flocs. The organometallic particulate floc is removed as alum water treatment residue (AWTR). Ideally, agglomeration of particles in water into flocs is by a four stage coagulation mechanism namely, double layer compression, sweep flocculation, adsorption and charge neutralization, and inter-particle bridging [8, 9].

$$Al_2(SO_4)_3.14H_2O + 3Ca(HCO_3)_2 \rightleftarrows Al(OH)_3\downarrow + 3CaSO_4 + 6CO_2 \quad (1)$$

The amphoteric hydroxide of aluminium allows for effective dissolution in acidic and alkaline mediums (Eq. (2) to (6)). However, due to the non-selective nature of dissolution agents such as sulphuric acid, nitric acid, hydrochloric acid and hydroxides of sodium and calcium for heavy metals and natural organic matter [10-12], secondary treatment is required.

Received July 14, 2019 **Accepted** September 29, 2019

† Corresponding author
Email: ektetteh34@gmail.com
Tel: +27-313732123 Fax: +27-866741148
ORCID: 0000-0003-1400-7847

acidic:

$$Al(OH)_3 + 3HCl \rightarrow AlCl_3 + 3H_2O \quad (2)$$

$$Al(OH)_3 + 3HNO_3 \rightarrow Al(NO_3)_3 + 3H_2O \quad (3)$$

$$2Al(OH)_3 + 3H_2SO_4 \rightarrow Al(SO_4)_3 + 6H_2O \quad (4)$$

alkaline

$$Al + 3H_2O + NaOH \rightarrow Na[Al(OH)_4] + \frac{3}{2}H_2 \quad (5)$$

$$2Ca^{2+} + 2Al(OH)_4 + 8H_2O \rightleftarrows Ca_3Al_2(OH)_{12} + 6H_2 \quad (6)$$

Sustainability requires meeting demands with progressively less deleterious impact to the environment. Water demand is under pressure with the rapid increase in population and as urbanization heightens. Consequently, global freshwater demand is expected to have a 55% increase from the current volume to 5,500 km^3 [13]. In meeting the potable water usage demand, AWTR is also expected to increase. It is therefore not feasible to continuously deposit AWTR in landfills, hydric and lagoons as they are deposited without any treatment [14, 15]. Therefore, efficient and sustainable management of generated AWTR in an eco-friendly and economical way is essential for the water sector and the environment. Recovery and reuse of AWTR is seen as the best sustainable management practice. Regenerating of the recovered coagulant residue for reuse can reduce commercial coagulant demand by (70%) and the disposal volume [16].

Other methods reported in literature for Al separation employ processes such as membrane size separation, resin adsorption and ion exchange dialysis (IED) [17]. Among them, the IED process deserves special attention owing to it being simple, energy saving and economical. The technique is useful in the recovery and concentration of metals through stoichiometric counter transport of ions by an electrochemical potential gradient [18]. The target ion of interest in the feed solution is separated from the donating ion in the sweep solution of high ionic strength by a cation exchange membrane.

Depending on the IED set-up, operating variables to establish recovery are but not limited to feed and sweep flowrates, membrane morphology and type, feed and sweep concentration, co-ion valency, pH and membrane type [19, 20]. Previous studies of IED that achieved a recovery of ≥ 70% Al^{3+} did not focus on independent and interactional effect of process variables and process optimization over a wide range of conditions [21, 22]. The use of the classical one factor at a time (OFAT) technique for modeling and optimization is obsolete and does not show interaction process factors to establish cause-effect relationships [23].

Interreactional effects for the considered system require advanced techniques to sequentially develop adequate functional relationship between desired response and the input factors. In this case, Design of Experiments (DOE) applies mathematical techniques to the statistical modeling and systematic analysis of a problem in order to sequentially develop adequate functional relationship between desired response and input [24, 25]. One of the tools is response surface methodology (RSM) which was originally built by Box and Wilson to improve yield in the chemical and other process industries [26, 27]. It is a multivariable processing system that uses reduced experimental runs to generate statistically acceptable second-order polynomial equations that contain the significant factors affecting the response and the main interacting factors [28]. The most common is the central composite design (CCD) with two notable classifications namely: face-centered CCD (FC-CCD) and rotable CCD [25]. Ooi et al. [29] applied CCD for the acidic recovery of alum from AWTR.

The knowledge on the use of FC-CCD in the study of aluminium permeation on a counter flow IED system is limited in literature. Therefore, this study aims to investigate systematically the effect of process variables on the permeation of aluminium. The FC-CCD was employed to expound on feed flow rate, sweep flow rate, feed concentration and sweep concentration interactions on Al-permeation. Mathematical models to predict the effect of the aforementioned factors on the response was generated. Also presented are 3D-surface plots for graphical visualization of the interactional effects of the factors.

2. Experimental

2.1. Materials

Analytical or higher grade chemicals [$Al_2(SO_4)_3.18H_2O$ (≥ 97%), HCl (≥ 36.5%)] and demineralized water (17.5 MΩ/cm) were used in the current study. The cation exchange membrane (Nafion 117) with strong sulfonic cation exchange groups with an equivalent weight of 1100 g and thickness of 177. 8 μm was purchased from Merck, South Africa. The membrane was purified prior to the experiment by the following procedure: immersion in demineralized water for 15 min, followed by leaching in 3% wt H_2O_2 at 60°C for 60 mins and rinsing with demineralized water at 25°C. Protonisation in 3% wt HCl at 90°C and 1% wt of the acid at 25°C for 60 min and 180 min, respectively was done. Intermediate rinsing with demineralized water for 15 min was performed for the two acid treatments. Final washing with demineralized water was done to conclude the 6 h activation process.

2.2. Ion Exchange Dialysis

The permeation study involves exchange of trivalent cation in the recycling feed vessel with monovalent cation in the recycling sweep vessel at a 2:1 volume ratio. Feed concentration, 100- 3,300 ppm the Al-acidic salt and Sweep concentration ranges of 0.25-1 N HCl was fed (max. flow rate = 2.6 mLs^{-1}) into the counter flow IED rig. Nafion 117 membrane with an active surface area of 205 cm^2 was clamped between the PVC made rig. The IED system integrated with the expected stoichiometric ion transport is shown in Fig. 1. The choice of low feed concentration (< 300 ppm) was based on surveyed Al-concentration in leachate and filtrate residue prior to a conventional ion exchange recovery process [30-32]. Using maximum Al-composition (> 2,500 ppm) in residue reported by Prakash et al. [21] and a mid-rate cut-off, 50% Al- permeation was selected by authors as a basis to conduct preliminary screening to determine maximum feed concentration. Operating the counter flow system at high HCl concentration (≥ 1 N) was avoided to

prevent osmotic dehydration of membrane gel structure, co-ion exclusion, reverse transport of target ions and osmotic transport [33]. Each experimental run was conducted for 24 h at a temperature of 22-25°C and the permeation was calculated according to Eq. (7).

$$Y_{24}(\%) = \frac{C_o - C_e}{C_o} \times 100 \quad (7)$$

where Y_{24} (%) is the percentage of aluminium permeation, C_o is the initial concentration of the Al in feed solution at t = 0 and C_e is the Al-concentration at t = 24 h.

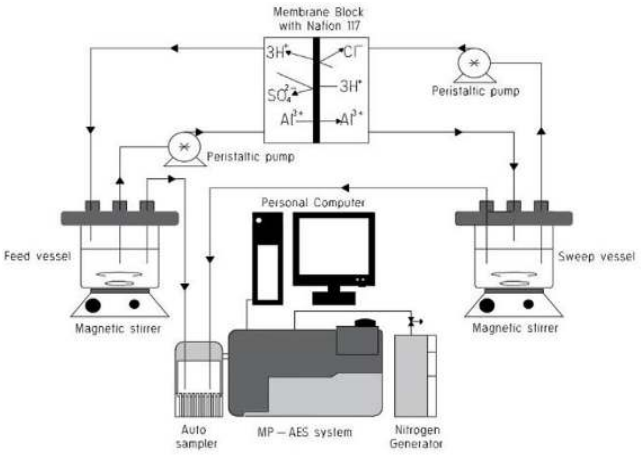

Fig. 1. Integrated IED system.

Periodic analysis of the target ion concentration for collected samples was carried out by the Agilent micro-plasma atomic emission spectrophotometer (MP-AES, MY 18379001) with optimized setting of wavelength 309.271 nm, 3 s read time, -10 viewing position and nebulizer flow of 0.9 l/min . Atomic emission wavelengths for detection of Al^{3+} was selected based on accuracy and repeatability of calibration curve for an R-square (0.9999) and percentage error relative standard deviation (5%). The MP-AES is only schematically connected and represented in Fig. 1. Calibration was done between 0-50 ppm Al and samples collected were diluted (5 to 100 times dilution) with 1% wt HNO_3 to volume prior to analysis.

2.3. Design Matrix

In this paper, face centred central composite design (FC-CCD) was used to study the impact of the operating conditions for Al-permeation. Design Expert software (Stat-Ease, Inc., Minneapolis, MN, USA, version 11) was used for regression analysis of experimental data and to plot response surface while ANOVA was used to estimate the statistical parameters. Four independent variables were chosen as A: feed concentration (X_1); B: feed flow rate (X_2); C: sweep concentration (X_3) and D: sweep flow rate (X_4). These factors were studied at three different normalized central representation levels coded as -1, 0, +1 corresponding to the minimum, central point and maximum for X factors ($-1 \leq X \leq +1$). The Al^{3+} in the feed vessel was selected as response of the system. The factors and their respective levels for the design matrix in actual and coded values are summarized in Table 1.The order of the runs was randomised to prevent systematic errors. The FC-CCD generated 30 experimental designed matrix classified with 16 cube points, 4 center points in the cube, 2 centre points in the axial direction and 8 axial points. The total of 6 replicated center points (cubic and axial) as proposed by the design software was for estimation of the pure error sum of squares.

3. Results and Discussion

3.1. One Factor at a Time (OFAT) Approach

The preliminary screening study was first carried to determine the maximum feed concentration and choose the appropriate ranges. This was done by changing the value of one variable at a time while keeping the other variables at a fixed condition (OFAT-approach). Fig. 2 shows the effect of low- high feed and sweep flowrates on the permeation of aluminium using a 1 N sweep concentration for high feed concentration. Using a low (25%) and high (85%) flowrate, feed and sweep flowrate conditions were set at (1) low feed flowrate and low sweep flowrate, (2) high feed flowrate and high sweep flowrate, (3) high feed flowrate and low sweep flowrate and (4) low feed flowrate and high sweep flowrate. Generally, permeation in Nafion 117 membrane on the counter current IED system by molar stoichiometry is in a 1:3 Al: H exchange. At 24 h, Al-permeation for 3,000 ppm feed concentration was below 50%. Thus, the ionic strength of the acid is not strong enough to establish the sufficient potential gradient for transport. The lowest Al-permeation of 37.6% for low feed and sweep flowrates was obtained for 3,000 ppm. The highest of 43% Al-permeation was recorded for high flow and sweep flowrates for the same sweep concentration at 3,300 ppm. Permeation study for 2,000 ppm feed was above 50% cut-off, hence was selected as the feed range.

Table 1. Independent Variables in Actual and Coded Levels

Independent variables	Symbol	Level		
		Low (-1)	Middle (0)	High (+1)
X1: Feed concentration (ppm)	A	100	1,050	2,000
X2: Feed flowrate (%)	B	25	55	85
X3: Sweep concentration (N)	C	0.25	0.625	1
X4: Sweep flow rate (%)	D	25	55	85

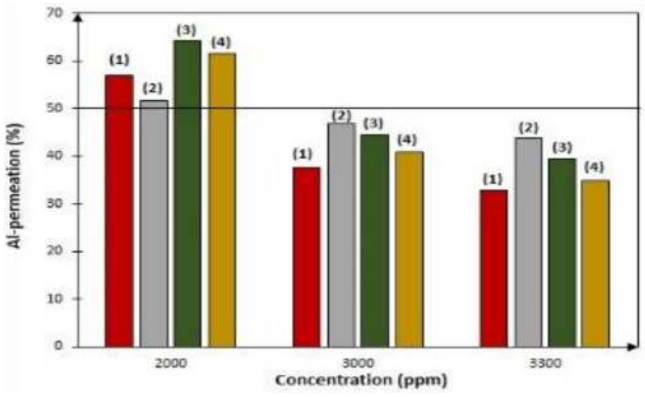

Fig. 2. OFAT permeation Cut-off for selected feed ranges.

3.2. ANOVA Analysis and Model Fitting

Data from the experiments conducted according to the design points were analyzed by the response surface regression procedure using the second-order polynomial equation (Eq. (8)) to evaluate the quality characteristic of the response as a function of the four independent factors:

$$y = \beta_o + \sum_{n=1}^{n} \beta_i x_i + \sum_{i=1}^{n} \beta_{ii} X_i^2 + \sum_{i}^{i<j,k} \sum_{j,k} \beta_{ijk} x_i x_j x_k + \varepsilon \quad (8)$$

Where y is the response/transmittance function; β_o is the offset term or intercept; β_i, β_{ii}, β_{ijk} denotes the regression coefficient for the linear, quadratic and interactive coefficients, respectively, ε is the random error and k is the number of variables studied. Per a unit increase in x, the coefficient for their non-interactions allows the estimation of the mean response when other factors are kept constant [34]. Analysis of variance (ANOVA) is part of the general linear model for partitioning and attribution of the total variability of experimental data into two parts: attribution to specific causes and ascription to chances in order to mimic the model [35]. Attributions to specific causes and chances are known as variation between the samples and variations within the samples, respectively. Table. 2 lists the results of the ANOVA and the *F*-test in order to evaluate the significance of the quadratic model.

The overall efficiency of the quadratic fit model's prediction and prediction variation is expounded by the coefficient of determination (R^2). Good model prediction efficiency should be close to 1. The Adjusted R^2 (Adj. R^2) and coefficient of variation (CV) also prominently defines the efficiency of predictions [34]. From Table 2, the R^2 at 24 h of 0.9568 is explicated with their respective model reproducibility (CV of 3.82%). A reproducible model has CV not greater than 10% [36]. In effect, 4.32% variations in the Al(III) are not associated to the four factors and explained by Y_{24} (Eq. (9)). A large difference (> 0.2) between the R^2 and Adj. R^2 implies that there is the least possibility that insignificant terms are included in the model. The increase in Adj. R^2 will result from model improvement with the inclusion of new terms or exclusion [37, 38]. An exemption of insignificant terms in the model is reflected by their low differences (0.0216) for Y_{24}. The Predicted R^2 (Pred. R^2) of 0.8646 shows a good agreement between the experimental data and predicted values for Al(III) permeation and goodness-of-fit of the regression. Table. 2, also depicts that here is 0.01% chance that a lack of fit F-value of this large (1,435.81) could occur due to noise. Similar trends of a significant model from the R^2 and Pred. R^2 with a difference less than 0.2 and a significant lack of fit has been reported [39-41].

The probability (*P*-value) was used to evaluate the model terms

Table 2. ANOVA of the Response Surface Quadratic Model Al(III) - Permeation At 24 h

Source	Sum of Squares	Degree of Freedom (DF)	Mean Square	F- Value	P- Value
Block	1.48	2	0.7395		
Model (Quadratic)	36.90	9	4.10	44.32	< 0.0001
A	15.17	1	15.17	164.01	< 0.0001
B	2.58	1	2.58	27.89	< 0.0001
C	8.19	1	8.19	88.54	< 0.0001
D	0.1030	1	0.1030	1.11	0.3054
AB	1.37	1	1.37	14.84	0.0012
AC	2.75	1	2.75	29.68	< 0.0010
A2	0.5765	1	0.5765	6.23	0.0225
B2	0.9059	1	0.9059	9.79	0.0058
C2	0.3441	1	0.3441	3.72	0.0697
Residual	1.67	18	0.0924		
Lack of Fit	1.67	15	0.1110	1435.81	< 0.0001
Pure Error	0.0002	3	0.0001		
Corr. Total	40.05	29			

R^2: 0.9568; Adj. R^2: 0.9352; Pred.R^2: 0.8646; Std. Dev.: 0.3042; CV= 3.82%

at 95% confidence level (denoted as $\alpha = 0.05$; $p > F$). Statistically, there exists a significant correlation between the response and each term, based on the *p*-value ≤ α. On other hand, where, p > α indicated that the relation between the response and the referenced term is not statistically significant one [42]. As shown in Table. 2, all the model terms are significant with $p < 0.05$, except D and C^2, which might not have high influence on the response. Model Y_{24} in Eq. (9) can be reduced to the expected model as represented in Eq. (10). Model term *A* in Eq. (9) has a negative coefficient and the vice versa in the latter. However, the inclusion of the D and C^2 terms increases the model prediction accuracy and therefore cannot be ignored. The D term cannot be ignored as it is further required in the typical operation of the counter flow IED system. A comparative account of predicted and actual plots as indicated in Fig. 3(a) and 3(b) for both models shows that the model Eq. (10) R^2 and Adj. R^2 values (Fig. 3(b)) are 1.16% and 0.91% less than the selected model Eq. (9). Also, model reproducibility, CV of 4.08% is higher. Both models are significant with slight variation.

selected model:

$$\sqrt{Y}_{24} = 4.81487 - 0.060\,x\,10^{-3}A + 93.732\,x\,10^{-3}B + 3729.57x\,10^{-3}C - 2.521\,x\,10^{-3}D - 0.010\,x\,10^{-3}AB + 1.163\,x\,10^{-3}\,AC - 5.08538E - 07A^2 - 0.639\,x\,10^{-3}B^2 - 2.52141C^2 \quad (9)$$

simplified model

$$\sqrt{Y}_{24} = 5.00650 + 0.244\,x\,10^{-3}\,A + 109.698\,x\,10^{-3}B + 577.807x\,10^{-3}C - 0.010\,x\,10^{-3}AB + 1.163\,x\,10^{-3}\,AC - 6.53283E - 07A^2 - 0.784\,x\,10^{-3}B^2 \quad (10)$$

Coefficients of the model terms are the expected changes in response per unit change in a factor when other factors are kept constant. The positive influencing terms on Al^{3+} permeation are limited to *B* and *C* only whilst the *A* and *D* have a negative influence on permeation. The model coefficients of the coded equation generated is presented in Fig. S1.

Fitting of significant factors was first done by the forward selection method [38, 43] and later inclusion of the D and C terms. The impact in order of ascendency for the single model is D < B < C < A and BD < AD < BC < CD < AB < AC for interacting factors and $D^2 < C^2 < A^2 < B^2$ for quadratic terms.

3.3. Model Validation and Verification

The normality probability of residuals and residuals versus predicted plots are used to evaluate the goodness-of-fit of the model. In a normality probability plot, the experimental data must follow a normal distribution with mean μ and variance σ^2 such that a plot of the theoretical percentiles of the normal distribution with the sampled percentiles should be approximately linear [44]. Data points that egress from a straight line indicates non-normality. The approximate linearity of the maximum colour points Fig. S2(a), supports the condition that the error term (ε), is normally distributed as it follows a straight line and high validity of the developed quadratic model [45]. Fig. S2(b), which is scatter plot of residuals and estimated response -Y_{24} shows the data points are non-linear with random scattering around the estimated regression line. In the presence of unequal error variances, observed responses shows no outliers as detection is within the boundary of ± 3.73.

3.4. Response Surface Analysis

Based on the effects of the four factors (A, B, C, D) at three levels, a 3D diagram with an integrated contour plots at the base Fig. 4(a)-(f) were obtained for responses of Al^{3+} permeation at 24 h. This helps to assess the correlative effect of the underlined factors on the response Y_{24} as generated with the model (Eq. (9)). To determine the optimum conditions of each factor for Al(III) permeation, the independent factors are held at 1,050 ppm A, 0.625 N C and 55% B and D.

Fig. 4(a), revealing the interaction between sweep slow and feed flow shows that decreasing the feed flowrate and increasing feed

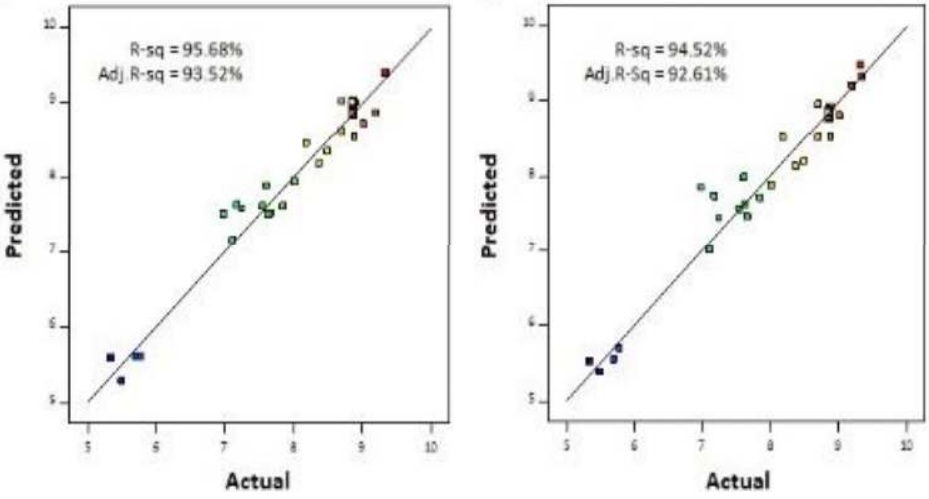

Fig. 3. Comparative plots. (a) Predicted vs Actual for Eq. (9), (b) Predicted vs Actual for Eq. (10).

concentration reduces the Al-permeation in the IED process. High Al-permeation (70-90 %) was observed for 100 ppm to > 1,100 ppm A and B > 45%. Also, 46-60% Y_{24} was recorded for 1,700-2,000 ppm A and 25% to > 47% B. The mutual interaction of the C with A and D depicts the extent of sweep effect of C on Y_{24}. In the AC interaction (Fig. 4(b)), increasing C, increases permeation as 65-80% was observed for 0.45-0.7 N HCl. The net sweep effect is almost linear for low feed concentration for > 0.7 N. The almost linear impact of sweep flowrate as demonstrated in Fig. 4(c), 4(d), and 4(e), indicates that sweep flowrate is the least important factor of the considered factors. Irrespective of the increase within the study range, a 61.82% ± 1.30 Al-permeation is achieved. Predicted response increases to about 75-77% before a decline at the operation ranges for the feed flowrate. Reducing the feed concentration increases the permeation from > 55% for 2,000 ppm to almost > 82% along the range study in Fig. 4d. Initially indicated with the almost linear effect of the sweep flow, a ratio 1:1.05 change for low permeation and high permeation of 1:1.09 at an 80% Y_{24} reference is observed. Increasing the feed flow and sweep concentration has an increasing effect on the response (Fig. 4(e)). Earlier in the Impact Pareto- diagram (Fig. S1), both B and C have a positive effect, hence their overall positive interactions.

3.5. Optimization and Validation Experiment

The desired goal for each factor and the response (y_i) is chosen during numerical optimization using the desirability function [d_i (y_i)] approach. The desirability function (range of $0 \leq d_i \geq 1$) combines all the goals in each response into individual desirability functions and then assemblage into an arithmetic or geometric mean [46, 47]. The suggested solution is expected to be close to or equal to 1. The possible goals which come with upper and lower limits as provided by the software are into five categories- minimum, maximum, within range, target and none. Optimized conditions under the specified curtailments were obtained at highest desirability of 1 for 1,540.70 ppm feed concentration, 63.5% feed flowrate and 47.6% sweep flowrates and sweep concentration of 0.7 N. The lower and upper weight of 1 and priority of 3 were assigned to all terms in this study. Desired goal for Al-permeation was set at a target of $\boldsymbol{Y_{24}}$ = 70%.

Additional 5 experiments were performed to confirm the accuracy of the predicted model and reliability of the optimum conditions and the results obtained are present in Table 3. It was deduced that, the predicted model values was in close agreement with the confirmation experimental run, with less than 2% variation.

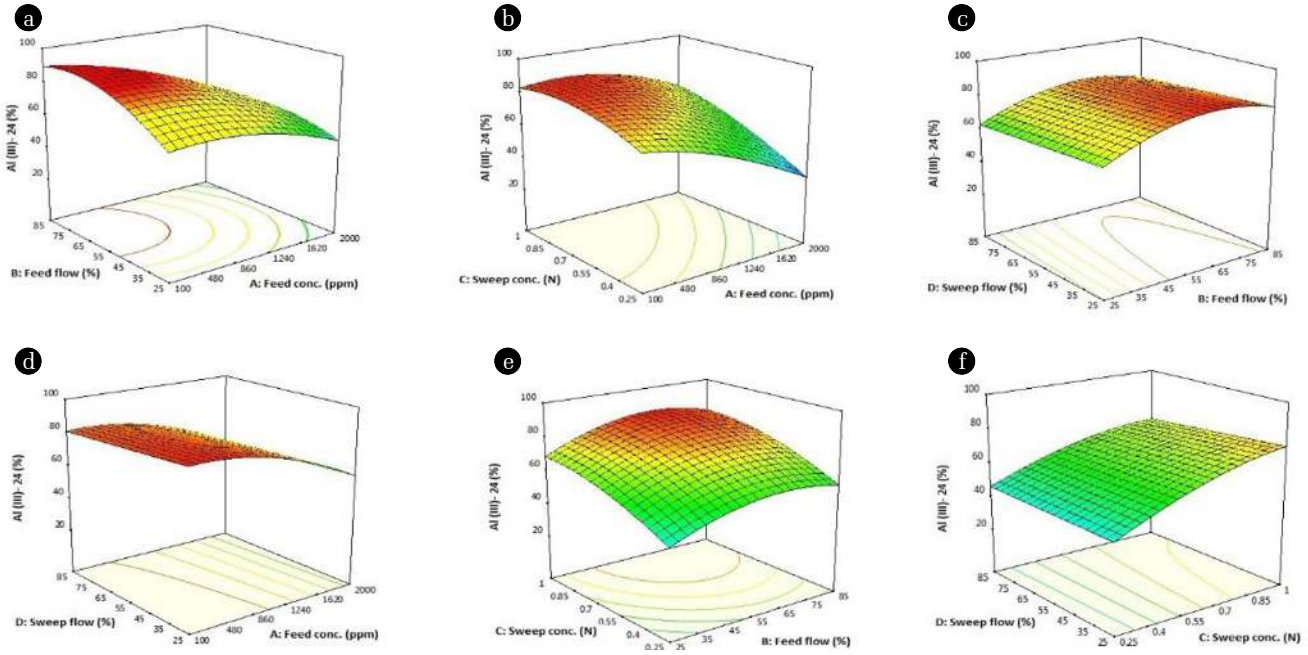

Fig. 4. Response surface plot for the correlative effects of: (a) Feed flow and Feed concentration.; (b) Sweep concentration and Feed concentration.; (c) Sweep flow and Feed flow; (d) Sweep flow and Feed concentration ; (e) Sweep concentration and Feed flow; (f) Sweep flow and Sweep concentration.

Table 3. Optimum Conditions for Target Recovery

Feed conc. (ppm)	Feed flowrate (%)	Sweep conc. (N)	Sweep flowrate (%)	Al-permeation (%)		Desirability
				Predicted	Observed	
1,540.70	63.5	0.7	47.6	70	68.77 ± 2.22	1

4. Conclusions

This study presented an evaluation and prediction of the independent and interactional effect of process variables on the Al-permeation for a counter flow IED system. Using FC-CCD response surface modeling analysis, a second-order quadratic model was generated. The experimental data obtained were well fitted on a predictive permeation model with a regression coefficient of R^2 = 0.9568. Confirmation experiments at optimum conditions gave a target Al-permeation of 69% as compared to the model prediction value of 70% at 1,540.70 ppm feed concentration, 63.5% feed flowrate and 47.6% sweep flowrates and sweep concentration of 0.7 N. In implementing a counter flow IED system, the feed concentration, feed flowrate and sweep concentration are the most determining factors. A non-decreasing and increasing effect is observed for sweep flowrates. Therefore, employing RSM to generate a predictive model and establish the interrelationship between the independent factors and the response serves as baseline for engineering design and scale-up of counter flow IEDs for Al-studies. However, aside the current studied flat sheet cell design, other membrane module design and flow schemes for IED Al-permeation can be considered.

Acknowledgments

The authors of this paper would like to express their sincere gratitude to the Water Research Commission – South Africa (WRC/2470) and National Research Fund-South Africa (UID-114058) for their grant support; facility and other resource support obtained from the Chemical Engineering Department-Durban University of Technology and the Process Engineering Department of Stellenbosch University.

References

1. Levett A, Gagen EJ, Diao H, et al. The role of aluminium in the preservation of microbial biosignatures. *Geosci. Front.* 2019;10:1125-1138.
2. Krishnan PK, Christy JV, Arunachalam R, et al. Production of aluminum alloy-based metal matrix composites using scrap aluminum alloy and waste materials: Influence on microstructure and mechanical properties. *J. Alloys Compd.* 2019;784:1047-1061.
3. Brandt MJ, Johnson KM, Elphinston AJ, et al. Chemical storage, dosing and control. Twort's Water Supply. 2017:513-552.
4. Kweinor Tetteh E, Rathilal S. Application of organic coagulants in water and wastewater treatment [Internet]. Org. Polym: IntechOpen; 2019 [cited 17 June 2019]. Available from: https://www.intechopen.com/online-first/application-of-organic-coagulants-in-water-and-wastewater-treatment.
5. Zueva SB. Current legislation and methods of treatment of wastewater coming from waste electrical and electronic equipment processing. *Waste Electr. Electron. Equip. Recycl.* 2018:213-240.
6. Brandt MJ, Johnson KM, Elphinston AJ, et al. Storage, clarification and chemical treatment. Twort's Water Supply. 2017:323-366.
7. Hamed MM, Hassan RS, Metwally SS. Retardation behavior of alum industrial waste for cationic and anionic radionuclides. *Process Saf. Environ. Prot.* 2019;124:31-38.
8. Tetteh EK, Rathilal S, Robinson K. Treatment of industrial mineral oil wastewater– Effects of coagulant type and dosage. *Water Pract. Technol.* 2017;12:139-145.
9. Matilainen A, Vepsäläinen M, Sillanpää M. Natural organic matter removal by coagulation during drinking water treatment: A review. *Adv. Colloid Interfac. Sci.* 2010;159:189-197.
10. Ramadan H, El Sayed AEA. Optimization of alum recovery from water treatment sludge-case study: Samannoud water treatment plant, Egypt. *Water Environ. J.* 2019:1-10.
11. Fouad MM, El-Gendy AS, Razek TMA. Evaluation of sludge handling using acidification and sequential aluminum coagulant recovery: Case study of El-sheikh zayed WTP. *J. Water Supply Res. Technol. - Aqua* 2017;66:403-415.
12. Ahmad T, Ahmad K, Alam M. Sustainable management of water treatment sludge through 3'R' concept. *J. Clean. Prod.* 2016;124:1-13.
13. Koleva MN, Styan CA, Papageorgiou LG. Optimisation approaches for the synthesis of water treatment plants. *Comput. Chem. Eng.* 2017;106:849-871.
14. Ahmad T, Ahmad K, Ahad A, et al. Characterization of water treatment sludge and its reuse as coagulant. *J. Environ. Manage.* 2016;182:606-611.
15. Xu Y, Chen T, Xu R, et al. Impact of recycling alum sludge on coagulation of low-turbidity source waters. *Desalin. Water Treat.* 2016;57:6732-6739.
16. Keeley J, Jarvis P, Judd SJ. An economic assessment of coagulant recovery from water treatment residuals. *Desalination* 2012;287:132-137.
17. Evuti AM, Lawal M. Recovery of coagulants from water works sludge : A review. *Adv. Appl. Sci. Res.* 2011;2:410-417.
18. Szczepanski P, Szczepanska G. Donnan dialysis-A new predictive model for non-steady state transport. *J. Membr. Sci.* 2017;525:277-289.
19. Strathmann H. Ion-exchange membrane separation processes. vol. 9. Amsterdam: Elsevier; 2004. p. 9-17.
20. Hichour M, Persin F, Molénat J, et al. Fluoride removal from diluted solutions by Donnan dialysis with anion-exchange membranes. *Desalination* 1999;122:53-62.
21. Prakash P, Hoskins D, SenGupta AK. Application of homogeneous and heterogeneous cation-exchange membranes in coagulant recovery from water treatment plant residuals using Donnan membrane process. *J. Membr. Sci.* 2004;237:131-144.
22. Prakash P, SenGupta AK. Selective coagulant recovery from water treatment plant residuals using donnan membrane process. *Environ. Sci. Technol.* 2003;37:4468-4474.
23. Adesina OA, Abdulkareem F, Yusuff AS, et al. Response surface methodology approach to optimization of process parameter for coagulation process of surface water using Moringa oleifera seed. South African *J. Chem. Eng.* 2019;28:46-51.
24. Nair AT, Makwana AR, Ahammed MM. The use of response surface methodology for modelling and analysis of water and wastewater treatment processes: A review. *Water Sci. Technol.*

2014;69:464-478.
25. Kleijnen JPC. Response surface methodology. *Int. Ser. Oper. Res. Manage. Sci*. 2015;216:81-104.
26. Box GEP, Wilson KB. On the experimental attainment of optimum conditions. *J. R. Stat. Soc. B.* 1951;13:1-38.
27. Kozan E, Koksoy O. A bayesian parameter estimation approach to response surface optimization in quality engineering. *Sak Univ. J. Sci.* 2019;23:767-74.
28. Balachandran M, Devanathan S, Muraleekrishnan R, et al. Optimizing properties of nanoclay–nitrile rubber (NBR) composites using Face Centred Central Composite Design. *Mater. Des.* 2012;35:854-862.
29. Ooi TY, Yong EL, Din MFM, et al. Optimization of aluminium recovery from water treatment sludge using Response Surface Methodology. *J. Environ. Manage.* 2018;228:13-9.
30. Petruzzelli D, Limoni N, Tiravanti G, et al. Aluminum recovery from water clarifier sludges by ion exchange. *React. Funct. Polym.* 1998;38:227-236.
31. Petruzzelli D, Volpe A, Di Pinto A, et al. Conservative technologies for environmental protection based on the use of reactive polymers. *React. Funct. Polym*. 2000;45:95-107.
32. Petruzzelli D, Volpe A, Limoni N, et al. Coagulants removal and recovery from water clarifier sludge. *Water Res*. 2000;34: 2177-2182.
33. Davis TA. Donnan Dialysis. Membr. Sep., vol. 2, Annandale-NJ: Academic Press; 2000. p.1701-177.
34. Montgomery DC. Design and analysis of experiments. 9th ed. John Wiley & Sons; 2017. p. 64-99.
35. Molugaram K, Rao GS. ANOVA (Analysis of Variance). *Stat. Tech. Transport. Eng*. 2017:451-462.
36. Nair AT, Ahammed MM. The reuse of water treatment sludge as a coagulant for post-treatment of UASB reactor treating urban wastewater. *J. Clean. Prod*. 2015;96:272-281.
37. Deb A, Ferdous J, Ferdous K, et al. Prospect of castor oil biodiesel in Bangladesh: Process development and optimization study. *Int. J. Green Energ.* 2017;14:1063-1072.
38. Schneider A, Hommel G, Blettner M. Linear regression analysis. Dtsch Aerzteblatt Online. 2010;107:776-782.
39. Torkaman R, Asadollahzadeh M, Torab-Mostaedi M. Effects of nanoparticles on the drop behavior in the Oldshue-Rushton extraction column by using central composite design method. *Sep. Purif. Technol.* 2018;197:302-313.
40. Marcos J, Fonseca L, Ramalho M, et al. Application of surface response analysis to the optimization of penicillin acylase purification in aqueous two-phase systems. *Enzyme Microbiol. Technol. 2*002;31:1006-1014.
41. Ghelich R, Jahannama MR, Abdizadeh H, et al. Central composite design (CCD)-Response surface methodology (RSM) of effective electrospinning parameters on PVP-B-Hf hybrid nanofibrous composites for synthesis of HfB2-based composite nanofibers. *Compos. Part B-Eng*. 2019;166:527-541.
42. Cox D. Statistical significance tests. *Diagn. Histopathol.* 2016;22:243-245.
43. Lalanne C, Mesbah M. Correlation, Linear Regression. Biostat Comput Anal Heal Data Using SAS. 2017:77-96.
44. Wulff SS. A First Course in Design and Analysis of Experiments. *Am. Stat*. 2003;57:66-67.
45. Tetteh E, Amano KOA, Asante-Sackey D, et al. Response Surface Optimisation of Biogas Potential in Co-Digestion of Miscanthus Fuscus and Cow Dung. *Int. J. Technol.* 2018;9:944-954.
46. Costa NR, Lourenço J, Pereira ZL. Desirability function approach: A review and performance evaluation in adverse conditions. *Chemom. Intell. Lab. Syst.* 2011;107:234-244.
47. Sadhukhan B, Mondal NK, Chattoraj S. Optimisation using central composite design (CCD) and the desirability function for sorption of methylene blue from aqueous solution onto Lemna major. *Karbala Int. J. Mod. Sci.* 2016;2:145-155.